EUROPEAN ORGANIZATION FOR NUCLEAR RESEARCH

CERN-EP/88-05
13 January 1988

MEASUREMENT OF THE STRONG-INTERACTION SHIFT AND BROADENING OF THE GROUND STATE OF THE $p\bar{p}$ ATOM[x)]

The ASTERIX Collaboration

M. Ziegler[2)], S. Ahmad[4)], C. Amsler[9)], R. Armenteros[1)], E.G. Auld[6)], D.A. Axen[6)], D. Bailey[1)], S. Barlag[1,*)], G.A. Beer[7)], J.C. Bizot[4)], M. Botlo[8)], M. Comyn[5)], W. Dahme[3,**)], B. Delcourt[4)], M. Doser[9)], K.D. Duch[2)], K.L. Erdman[6)], F. Feld-Dahme[3)], U. Gastaldi[1)], M. Heel[2,***)], B. Howard[6)], R. Howard[6)], J. Jeanjean[4)], H. Kalinowsky[2)], F. Kayser[2,†)], E. Klempt[2)], C. Laa[8)], R. Landua[1)], G.M. Marshall[7)], H. Nguyen[4)], N. Prevot[4)], J. Riedlberger[9)], R. Rieger[2)], L.P. Robertson[7)], C. Sabev[††)], U. Schaefer[3)], O. Schreiber[2,†††)], U. Straumann[2)], P. Truoel[9)], H. Vonach[8)], P. Weidenauer[2)], B.L. White[6)] and W.R. Wodrich[3,+)]

ABSTRACT

The K_α X-rays from $p\bar{p}$ atoms formed in H_2 gas at normal temperature and pressure are unambiguously identified by coincidences with L X-rays populating the 2P level. Background due to inner bremsstrahlung is suppressed by selecting events annihilating into neutral final states only. The K_α line is observed with a significance of more than 25 standard deviations at an energy of 8.67(15) keV. From fits to the K_α line we obtain a strong-interaction shift and width of the 1S level, averaged over the unresolved spin singlet and triplet contributions, of $\Delta E + i\,\Gamma/2 = [-0.70(15) + i\,0.80(20)]$ keV.

(Submitted to Physics Letters B)

---

1) CERN, Geneva, Switzerland
2) University of Mainz, Fed. Rep. Germany
3) University of Munich, Fed. Rep. Germany
4) LAL, Orsay, France
5) TRIUMF, Vancouver, Canada
6) University of British Columbia, Vancouver, Canada
7) University of Victoria, Canada
8) University of Vienna, Austria
9) University of Zurich, Switzerland
x) This work comprises part of the thesis (D77) of M. Ziegler
*) Present address: Max Planck Institute, Munich, Fed. Rep. Germany
**) Present address: LeCroy Research Systems, Geneva, Switzerland
***) Present address: Boehringer Ingelheim, Fed. Rep. Germany
†) Present address: Volkshochschule Hanau, Fed. Rep. Germany
††) Visitor at CERN, Geneva, Switzerland
†††) Present address: Toshiba Munich, Fed. Rep. Germany
+) Present address: Schott Glaswerke, Mainz, Fed. Rep. Germany

The experimental determination of the strong-interaction shift and width of the 1S ground state of antiprotonic hydrogen atoms is of considerable interest since it measures the nucleon–antinucleon interaction in the S-wave at threshold. Several theoretical models [1] agree in predicting a negative shift ΔE (resulting in less binding) and a width Γ for the 1S state of about $\Delta E + i\,\Gamma/2 = [-0.5 + i\,0.7]$ keV. The splitting between the spin singlet and triplet ($^1S_0$ and $^3S_1$) sublevels and the difference of their hadronic widths are both expected [1] to lie in the range 0.1–0.3 keV. The shift and width of the 1S level can be determined by detecting the K X-ray lines of the $p\bar{p}$ atom and measuring their energies and their broadening ($nP \rightarrow 1S$ transitions with QED predictions for the energies [2] of $K_\alpha = 9.37$ keV, $K_\beta = 11.11$ keV, $K_\infty = 12.49$ keV).

The $p\bar{p}$ atom itself is the source of two kinds of background when it annihilates. Charged particles accelerated in the annihilation emit inner bremsstrahlung radiation with a sizeable yield in the X-ray energy region below 10 keV. Gamma-rays from the decay of π^0's or η's can scatter in the active material of the X-ray detector and simulate the absorption of an X-ray. These backgrounds can be minimized by selecting annihilation final states without charged particles and by using a gaseous detector with a minimum of material in the active volume.

Previous attempts to observe, with Si(Li) detectors [3], K X-rays from $p\bar{p}$ atoms formed in liquid hydrogen failed because of a high Compton background and the very low yield of K X-rays. An experiment using a H_2 gas target at 4 atm surrounded by a multiwire proportional counter [4] observed L X-ray transitions ($nD \rightarrow 2P$) with a yield of $6 \pm 3\%$ [5] and established a lower limit for the hadronic width of the 2P level $\Gamma_{had} \geq 10\Gamma_{rad}$. Early results from the Low-Energy Antiproton Ring (LEAR) experiments gave evidence for the observation of K-line transitions. The individual K lines were, however, not resolved [6] or the data suffered from large background contributions [7]. In this letter we report on the analysis of data collected with the ASTERIX detector [8] in 1986 using the 105 MeV/c beam at LEAR. The emphasis is on the unambiguous identification of the K_α line, the discussion of background sources, and the physical information that can be extracted from the fit to the K_α signal. An analysis of the K, L and M line intensities in single X-ray and in X-ray coincidence spectra, giving information about the $p\bar{p}$ atomic cascade in gas at NTP, and a detailed analysis of the inner bremsstrahlung process will be the subjects of subsequent papers.

The measurements were performed at LEAR in 1986 using the ASTERIX spectrometer with a dedicated trigger in 13 beam spills each of 1 h duration. The beam momentum was 105 MeV/c with a typical intensity of 70,000 $\bar{p}$/s. The antiprotons were moderated and stopped in the centre of a cylindrical H_2 gas target [L = 90 cm, R = 8 cm] at NTP where they formed $p\bar{p}$ atoms. The stop distribution was measured by reconstructing vertices of events with two or more charged particles in the final state; it was centred in the target and had a width of 13 cm FWHM along the beam axis (i.e. z direction) and 6 cm FWHM in the transverse plane. The target and the central detector are surrounded by seven cylindrical multiwire proportional chambers (MWPCs) and a solenoid providing a 0.8 T field. The momentum of charged tracks is measured over a solid angle of about 65% of 4π.

The central detector is a cylindrical X-ray drift chamber (XDC) [9]; it is separated from the H_2 gas target region by a 6 μm thick aluminized Mylar window, which is set to high negative voltage to establish the radial drift field towards the sense wires. Figure 1 shows the geometry of the target and the counter with the arrangement of the 90 sense wires and the 270 field wires defining 90 drift cells. The counter gas (50/50 Ar/C_2H_6) and the hydrogen target gas are continuously flushed to avoid mutual contamination. The chamber is operated at a gas gain of about 10^5. The signals at both ends of the 90 sense wires are sampled by 6-bit flash analog-to-digital converters (FADCs) with a known non-linear response covering a dynamical range from 0.3 to 25 keV [10]. The history of the last 4 μs is recorded in a cyclic memory in 32 ns bins. The leading edge of each pulse is digitized with 4 ns accuracy.

The distinctive features of the X-ray detector are:

i) high angular acceptance (90% of 4π);

ii) low-energy threshold due to the thin Mylar window between target and detector (detection efficiency greater than 5% between 1.0 and 16 keV);

iii) three-dimensional localization of the X-ray conversion point by wire number (ϕ), drift-time (r), and charge division (z) ($\Delta\phi$ = 21 mrad, Δr = 500 μm, Δz = 2 cm);

iv) low mass due to the gaseous detector.

Figure 2 shows an event with a triple coincidence of detected X-rays from a $p\bar{p}$ atom annihilating without charged particles traversing the counter gas.

Two radioactive sources, ^{57}Co and ^{54}Mn, positioned along the detector axis were used for energy calibration in beam-off conditions. They were used to determine the energy resolution and the overall response of the system, including amplification at the wire and in the preamplifiers, and the FADC response and its linearization function. The response function is known with an accuracy of ± 0.12 keV at 8.7 keV. Figures 3a and 3b show the calibration lines from ^{54}Mn and ^{57}Co after correction with the response function.

The in-beam calibration was provided by the L_α line of the $p\bar{p}$ atom (E = 1.734 keV)—which is singled out of the L line pattern by requiring in coincidence X-rays from the M series—and the 5.5 keV line of a ^{54}Mn source. During the run period the source was screened to illuminate only the downstream part of the 90 sense wires. Hence our 5.5 keV in-beam calibration was restricted to the downstream end of the target. The resolution and the gain within a spill and between different run periods were checked and remained constant. The detection efficiency calculated from the measured $\bar{p}$ stop distribution and assuming isotropic X-ray emission is shown in fig. 3c. Absorption in the Mylar foil, transmission through the counter gas, the requirement of a fiducial volume inside the XDC (z = -25 to 20 cm, $8.0 \leq r \leq 12.2$ cm), and the software cuts described below were taken into account. In order to veto events with charged particles the trigger required for each event at least one X-ray candidate present in the XDC and no hits in the two innermost MWPCs (covering a solid angle of about 90% of 4π). It selected 2×10^6 events in a total of about 3×10^9 antiprotons stopping in the target.

In the first step of the off-line analysis, events with obvious charged particles in the XDC were eliminated, leaving 710,000 events. The following additional criteria had to be fulfilled for an XDC pulse to be accepted as an X-ray:

i) a pulse shape compatible with that of X-rays from radioactive sources;

ii) a primary electron cloud contained in exactly one of the 90 drift cells ;

iii) a conversion radius between r = 8 cm (Mylar foil) and r = 12.2 cm;

iv) a position along the beam axis between -25 cm (upstream) and + 20 cm (downstream).

After application of these cuts 480,000 events were retained with exactly one X-ray, 9,000 events with two coincident X-rays, and 110 events with three coincident X-rays. Figure 4a shows the X-ray energy spectrum of all events. The prominent peak at low energies is due to the L X-ray series (E = 1.73–3.11 keV). The M lines (E = 0.5–1.3 keV) are detected with much lower efficiency and contribute to the low-energy tail of the L_α line without being resolved. The structure in the region between 7 and 13 keV is interpreted as the unresolved K lines sitting on some background. To make the signal more visible the scale of fig. 4a has been enlarged by a factor of 100 for energies above 4 keV. Since the detection efficiency (40–10% between 7 and 13 keV) is comparable to that of L lines, this low yield shows the dominance of annihilation over radiative transitions from the nP levels.

The main sources of background are

i) internal bremsstrahlung from events with charged particles escaping detection in the XDC (with an energy dependence 1/E, important below 10 keV),

ii) argon fluorescence (contributing at 3 keV),

iii) Compton scattering (giving a distribution slowly decreasing with energy, important above 5 keV).

The interpretation of the structure in the K line region is greatly facilitated by considering events with two coincident X-rays. They allow, in particular, selection of the K_α line out of the K series by requiring an L X-ray in coincidence with it. The background under the K lines is not correlated to the $p\bar{p}$ atomic cascade and hence is strongly reduced in the coincidence spectrum. Figure 4b shows the coincident X-ray spectrum. The peak in the 7.5 to 10 keV region has a significance of 25 standard deviations and is observed in coincidence with L lines, as expected for the K_α line.

Clear evidence that this peak is due to the K_α line stems from three additional experimental facts unique to our experiment:

i) The source of the X-rays is located in the centre of the H_2 target; the distribution of X-ray conversion points along the beam axis (fig. 5) is peaked at the centre of the target and is correlated with the $\bar{p}$ stop distribution. Figure 6 shows the distribution of the radial conversion points for X-rays in the L_α and the K_α region exhibiting a characteristic rise towards small radii, i.e. near to the target, consistent with the expected attenuation length. This proves that the X-rays originate from inside the target and excludes X-ray background from the walls of the X-ray detector or from a source outside the active volume of the XDC.

ii) X-rays in the K_α energy window are only coincident with the L lines. Figure 4c shows the energy spectrum of X-rays coincident with X-rays in the K_α region, displaying the L series. If the K_α peak were due to other exotic atoms formed with contaminations of the H_2 target, the lines in coincidence with X-rays in the K_α region would not give the distinct L line pattern of the $p\bar{p}$ atom at the correct energy. In addition, the different L line contributions agree quantitatively with those derived from the inclusive X-ray spectrum.

iii) We observe triple coincidences of M–L_α–K_α X-rays. Their rate is in agreement with expectations from the observed number of M–L_α and L_α–K_α double coincidences. The energy pattern of M, L_α, and K_α lines of the $p\bar{p}$ atom is unique and cannot be faked by other exotic atoms.

The observed K_α peak is noticeably broader than the energy resolution of our detector at 8.7 keV, indicating substantial hadronic broadening of the 1S state. The interpretation of this broadening is complicated by the possible splitting of the singlet and triplet components of the ground state. Annihilation into only neutral pions in coincidence with a K_α X-ray picks out the singlet state ($J^{PC} = 0^{-+}$) because of C-parity conservation, so we expect a large contribution from the singlet state to the observed K_α line. However, neutral annihilations involving neutral kaons or radiative decays may proceed from the triplet state as well; their relative contribution is unknown but small.

Since the broadening is much larger than the predicted singlet–triplet splitting [1] we have fitted the K_α peak to a single line. The line shape of atomic transitions into a broad state calculated by Ericsson and Hambro [11] was used. The shape function was multiplied by the energy-dependent detection efficiency and convoluted with a Gaussian (describing the detector resolution). The known experimental resolution at 8.7 keV ($\sigma = 1.00 \pm 0.17$ keV) was imposed. The complete X-ray spectrum of fig. 4c was fitted using the minimization program MINUIT [12] . In addition to the K_α line, the following contributions were taken into account:

i) two Gaussian functions representing the observed L_α and the argon fluorescence line;

ii) the energy spectrum of X-rays accompanied by argon fluorescence;

iii) the spectrum of inner bremsstrahlung [13] from charged pions escaping detection outside the XDC.

The Compton background was found to be negligible. The fit result is shown in fig. 7. We obtained for the energy and the width of the 1S level:

$$E(K_\alpha) = 8.67 \pm 0.15 \text{ keV}$$

$$\Gamma(K_\alpha) = 1.60 \pm 0.40 \text{ keV} \ .$$

A value of 1.04 was obtained for χ^2/N_f. The error of the energy measurement comes from the statistical error (±70 eV) and the error in energy calibration (±125 eV). We note that the energy dependence of the detection efficiency shifts the observed peak position towards lower energies. Without a strong-interaction shift the K_α line energy would be 9.37 keV. Leaving the experimental resolution as a free parameter, the fit gives a resolution of 1.2 ± 0.2 keV and a width within the error quoted above.

It is necessary to stress the dependence of the fitted K_α line position on the correct theoretical line shape for such a substantially broadened 1S level. The large width of the K_α line is not caused by gain variations of the detector, since the width of the L_α line (σ = 0.26 keV at 1.73 keV), observed under the same conditions in coincidence with M X-rays, is compatible with the nominal detector resolution at that energy.

In summary, we conclude that the strong broadening of the K_α line is due to the hadronic interaction, and it contributes a shift and width to the ground state of the $p\bar{p}$ atom of

$$\Delta E + i\Gamma/2 = [-0.70(15) + i\,0.80(20)] \text{ keV} \ .$$

These values are in agreement with the results of models for the $p\bar{p}$ interaction at low energies [1] and the energy shift agrees with preliminary results from other LEAR experiments [14].

The ϱ parameter is defined by the ratio between the real and the imaginary part of the forward $p\bar{p}$ scattering amplitude. At rest it is given by the ratio $\varrho = 2\,\Delta E/\Gamma$. From our measurement we obtain $\varrho = -0.88(31)$, adding information to the behaviour of the ϱ parameter measured in $p\bar{p}$ elastic scattering at low energies [15]. However, it is to be remarked that the spin singlet-triplet composition of the K_α line coincident with neutral annihilations may be different from that contributing to the elastic-scattering forward amplitude.

In conclusion, we have reported the direct observation of the K_α line of the $p\bar{p}$ atom, which is unambiguously identified by requiring L X-rays in coincidence. No background from higher K transitions is present and therefore no assumptions about their relative yields — depending on cascade calculations — enter the fit. Our unique identification of the K_α line is also important for the interpretation of bumps observable in other experiments on protonium, featuring better energy resolution but less possibilities of identifying the nature of broad structures.

Acknowledgements

We are indebted to the LEAR staff for the quality of the 105 MeV/c beam. This work was supported by the Deutsches Bundesministerium für Forschung und Technologie, by the Institut National de Physique Nucléaire et de Physique des Particules, by the Schweizer Nationalfond, by the Österreichische Nationalfond, and by the Natural Sciences and Engineering Research Council of Canada.

REFERENCES

[1] R.A. Bryan, and R.J.N. Phillips, Nucl. Phys. **B5** (1968) 201.
O.D. Dalkarov and V.M. Samoilov, JETP Lett. **16** (1972) 249.
I.S. Shapiro, Phys. Rep. **35** (1978) 129 and references therein.
W.B. Kaufmann, Phys. Rev. **C19** (1979) 440.
A.M. Green and S. Wycech, Nucl. Phys. **A377** (1982) 441.
J.M. Richard and M.E. Sainio, Phys. Lett. **B110** (1982) 349.
M.A. Alberg et al., Phys. Rev. **D27** (1983) 536.
B. Moussallam, Z. Phys. **A325** (1986) 1.

[2] S. Caser and R. Omnès, Phys. Lett. **B39** (1972) 369.

[3] M. Izycki et al., Z. Phys. **A297** (1980) 1.
J.R. Lindemuth et al., Phys. Rev. **C30** (1984) 1740.

[4] U. Gastaldi et al., Nucl. Instrum Methods **156** (1978) 257.

[5] E.G. Auld et al., Phys. Lett. **B77** (1978) 454.

[6] S. Ahmad et al., Phys. Lett. **B157** (1985) 333.

[7] T.P. Gorringe et al., Phys. Lett. **B162** (1985) 71.

[8] The ASTERIX Collaboration, The ASTERIX spectrometer, to be submitted to Nucl. Instrum. Methods.

[9] U. Gastaldi, Nucl. Instrum. Methods **157** (1978) 441.
U. Gastaldi et al., Nucl. Instrum. Methods **176** (1980) 99.

[10] B.J. Hallgren and M. Rijssenbeck, CERN Internal Note UA1 TN85-71 (1985).

[11] T.E.O. Ericsson and L. Hambro, Ann. Phys. **107** (1977) 44.

[12] F. James and M. Roos, MINUIT User Guide, CERN Program Library D506.

[13] U. Schaefer, Dissertation, Universität München (1987).

[14] For reviews of preliminary results, see, for example:
E. Klempt *in* Antiproton 86 (World Scientific, Singapore, 1987), ed. S. Charalambous.
L. Simons, *in* Proc. IVth LEAR Workshop, Villars-sur-Ollon, 1987 (Gordon and Breach, London and New York, 1988), p. 703.

[15] W. Brückner et al., Phys. Lett. **B158** (1985) 180.

Figure captions

Fig. 1 Side and transverse views of the ASTERIX target and X-ray drift chamber (XDC).

Fig. 2 Real event with three detected X-rays in coincidence in the XDC and without charged particles produced in $p\bar{p}$ annihilation.

Fig. 3 a) Calibration line from ^{54}Mn (5.5 keV and escape peak at 2.5 keV) after correction with the response function.

b) Calibration lines from ^{57}Co (6.5 keV and 14.4 keV) after correction with the response function.

c) Detection efficiency of the XDC with software cuts as described in the text.

Fig. 4 a) X-ray energy spectrum of all events. The dominant signal at 1.5–3 keV is due to the L series from the $p\bar{p}$ atom. The region above 4 keV is scaled by a factor of 100.

b) X-ray energy spectrum of events containing two coincident X-rays. Only the X-ray with the higher energy is histogrammed. The region above 2.5 keV is scaled by a factor of 20, displaying the K_α line over a small background.

c) X-ray energy spectrum of events containing two coincident X-rays. Only X-rays coincident with an X-ray in the K_α region [6.4–10.4 keV] are histogrammed. The structure at low energies is the full L series of the $p\bar{p}$ atom.

Fig. 5 Distribution of X-ray absorption points along the beam axis.

Fig. 6 Radial distribution of the X-ray absorption points.

Fig. 7 K_α line of $p\bar{p}$ atoms with only neutrals in the annihilation final state and fit to the line.

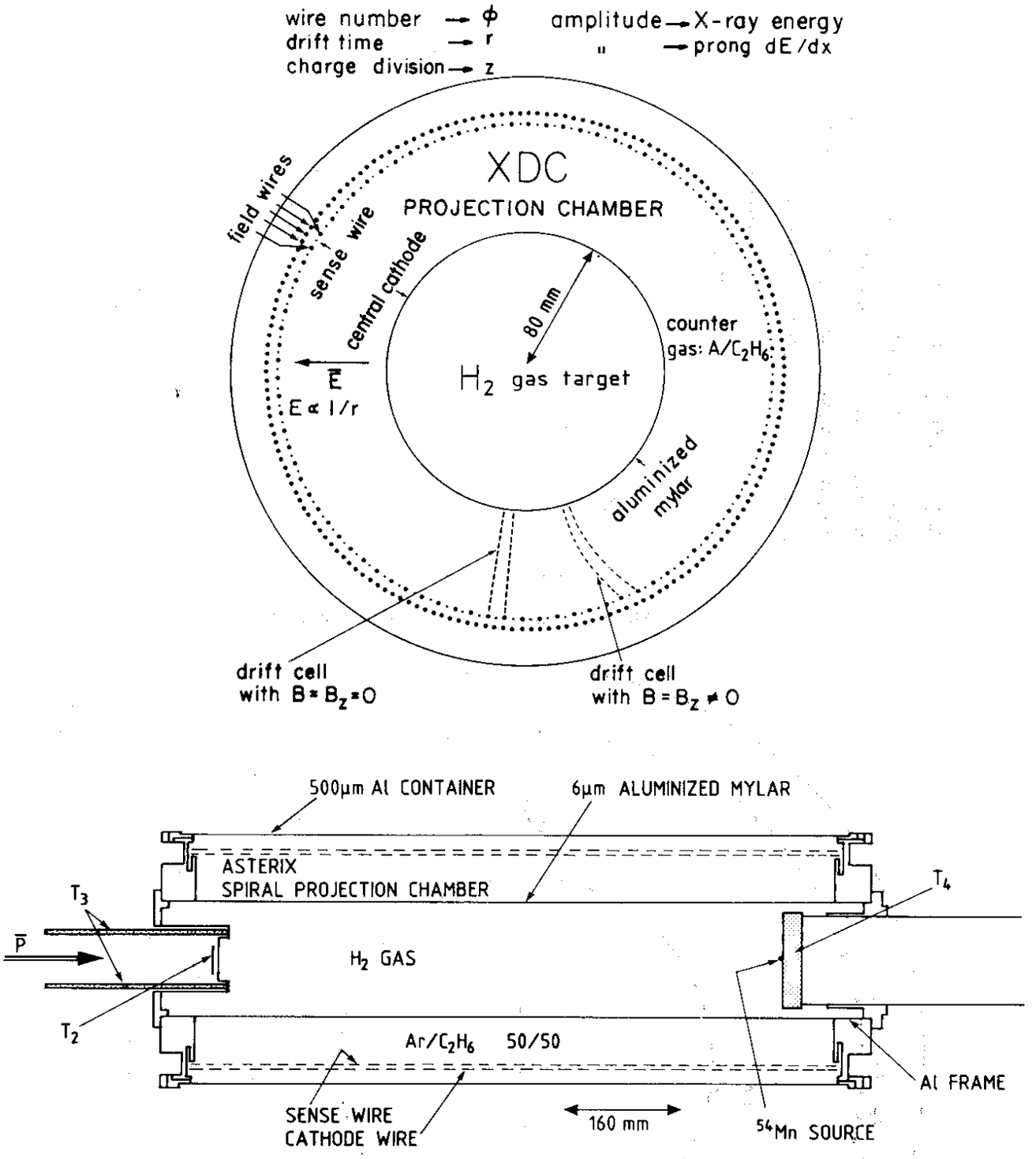
wire number → φ
drift time → r
charge division → z
amplitude → X-ray energy
" → prong dE/dx
XDC
PROJECTION CHAMBER
field wires
sense wire
central cathode
80 mm
counter
gas: A/C2H6
H2 gas target
E
E ∝ 1/r
aluminized mylar
drift cell
with B = Bz = 0
drift cell
with B = Bz ≠ 0
500μm Al CONTAINER
6μm ALUMINIZED MYLAR
ASTERIX
SPIRAL PROJECTION CHAMBER
T3
T4
P
H2 GAS
T2
Ar/C2H6 50/50
Al FRAME
SENSE WIRE
CATHODE WIRE
160 mm
54Mn SOURCE

Fig. 1

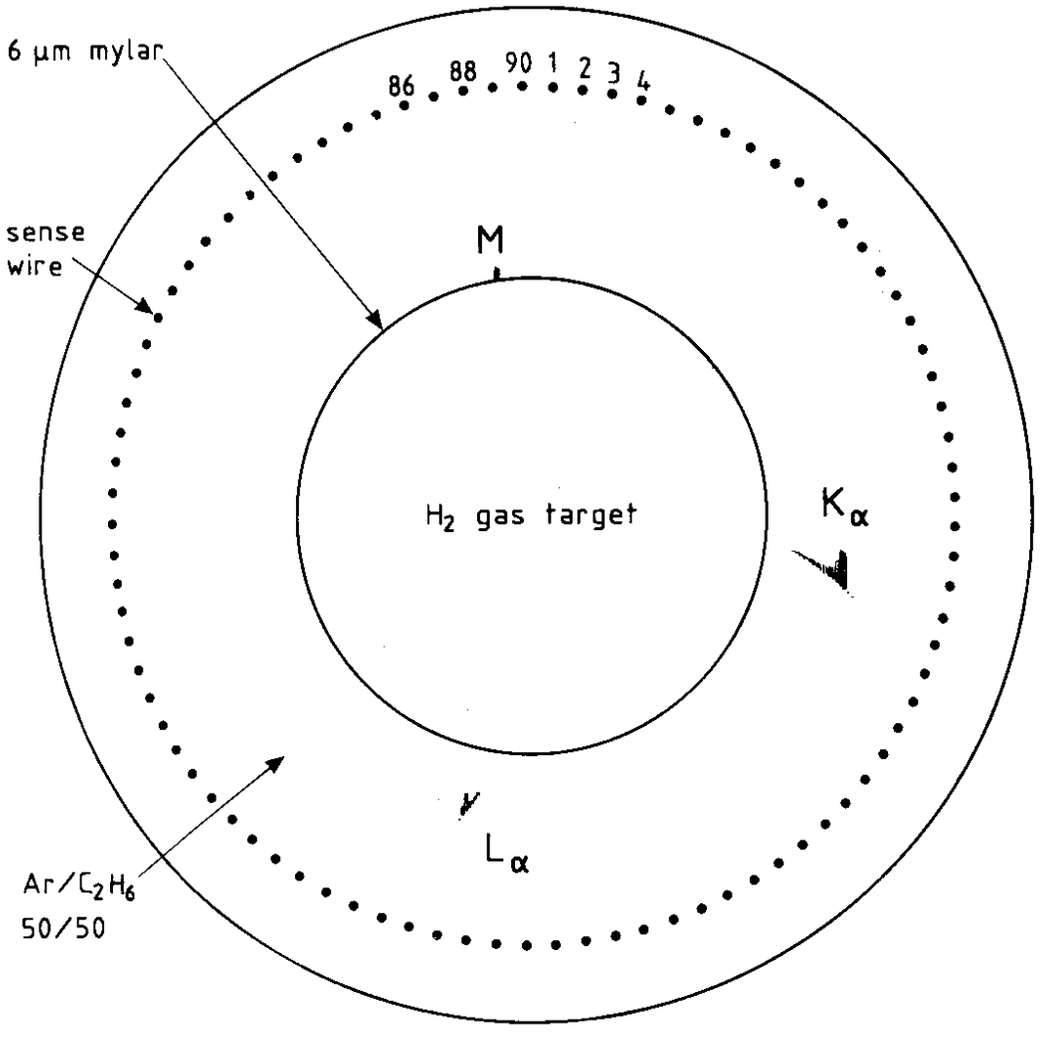

ASTERIX (PS 171)

Spiral Projection Chamber and
X-Ray Drift Chamber (SPC-XDC)
event visualization in the r Φ projection
Event: $p\bar{p} \rightarrow$ 3 X-rays +
all neutrals
annihilation

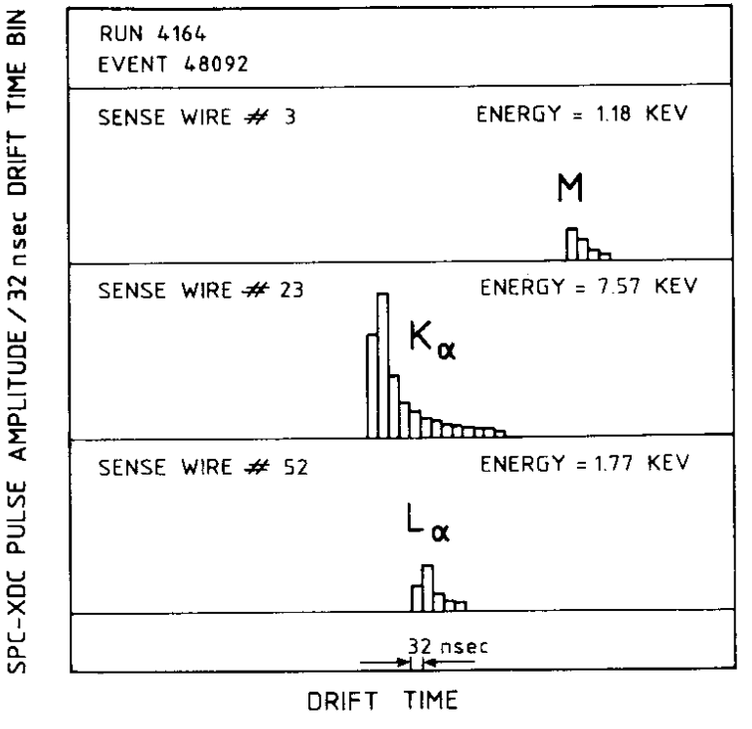

Fig. 2

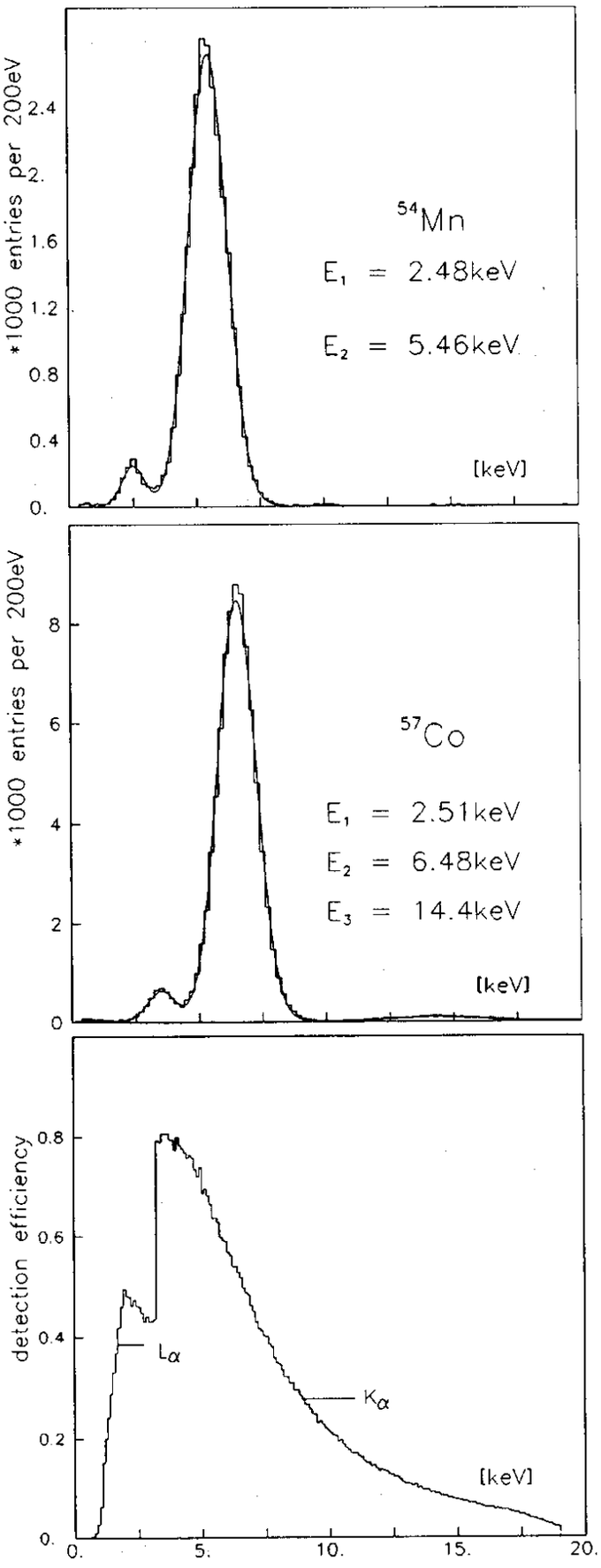
*1000 entries per 200eV
2.4
2.
1.6
1.2
0.8
0.4
0.
^{54}Mn
E_1 = 2.48keV
E_2 = 5.46keV
[keV]
*1000 entries per 200eV
8
6
4
2
0
^{57}Co
E_1 = 2.51keV
E_2 = 6.48keV
E_3 = 14.4keV
[keV]
detection efficiency
0.8
0.6
0.4
0.2
0.
Lα
Kα
[keV]
0.
5.
10.
15.
20.

Fig. 3

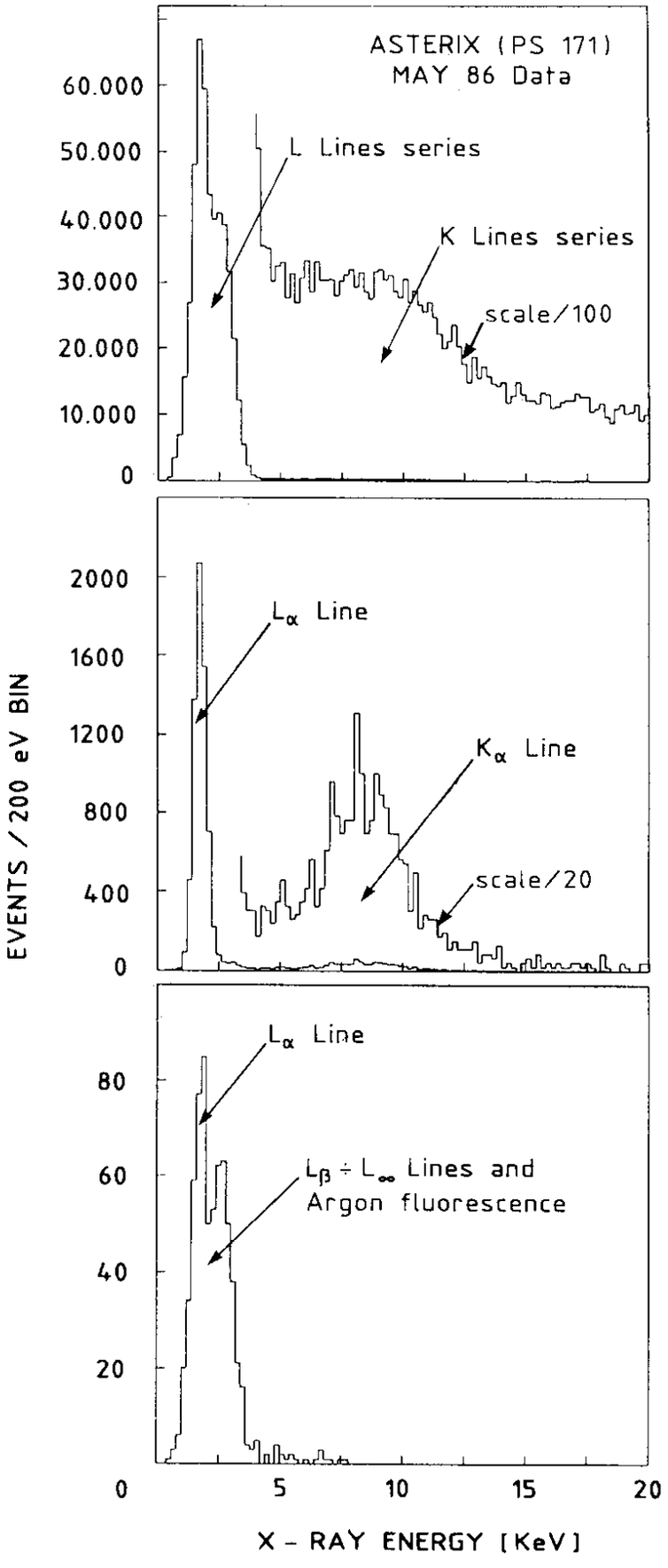
ASTERIX (PS 171)
MAY 86 Data
L Lines series
K Lines series
scale/100
L_α Line
K_α Line
scale/20
L_α Line
$L_\beta \div L_\infty$ Lines and
Argon fluorescence
60.000
50.000
40.000
30.000
20.000
10.000
0
2000
1600
1200
800
400
0
80
60
40
20
0
5
10
15
20
EVENTS / 200 eV BIN
X - RAY ENERGY [KeV]

Fig. 4

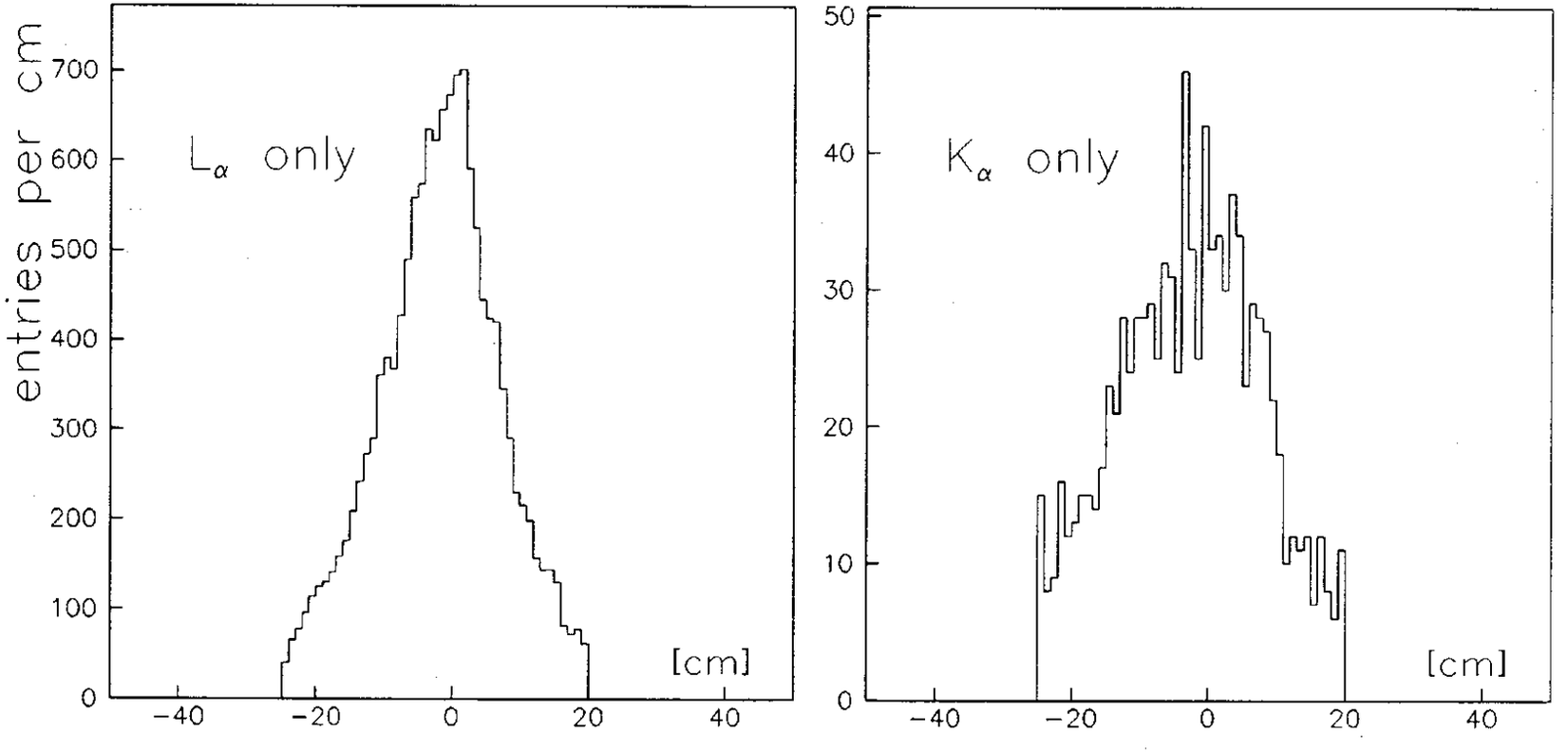
entries per cm
700
600
500
400
300
200
100
0
L_α only
[cm]
−40
−20
0
20
40
50
40
30
20
10
0
K_α only
[cm]
−40
−20
0
20
40

Fig. 5

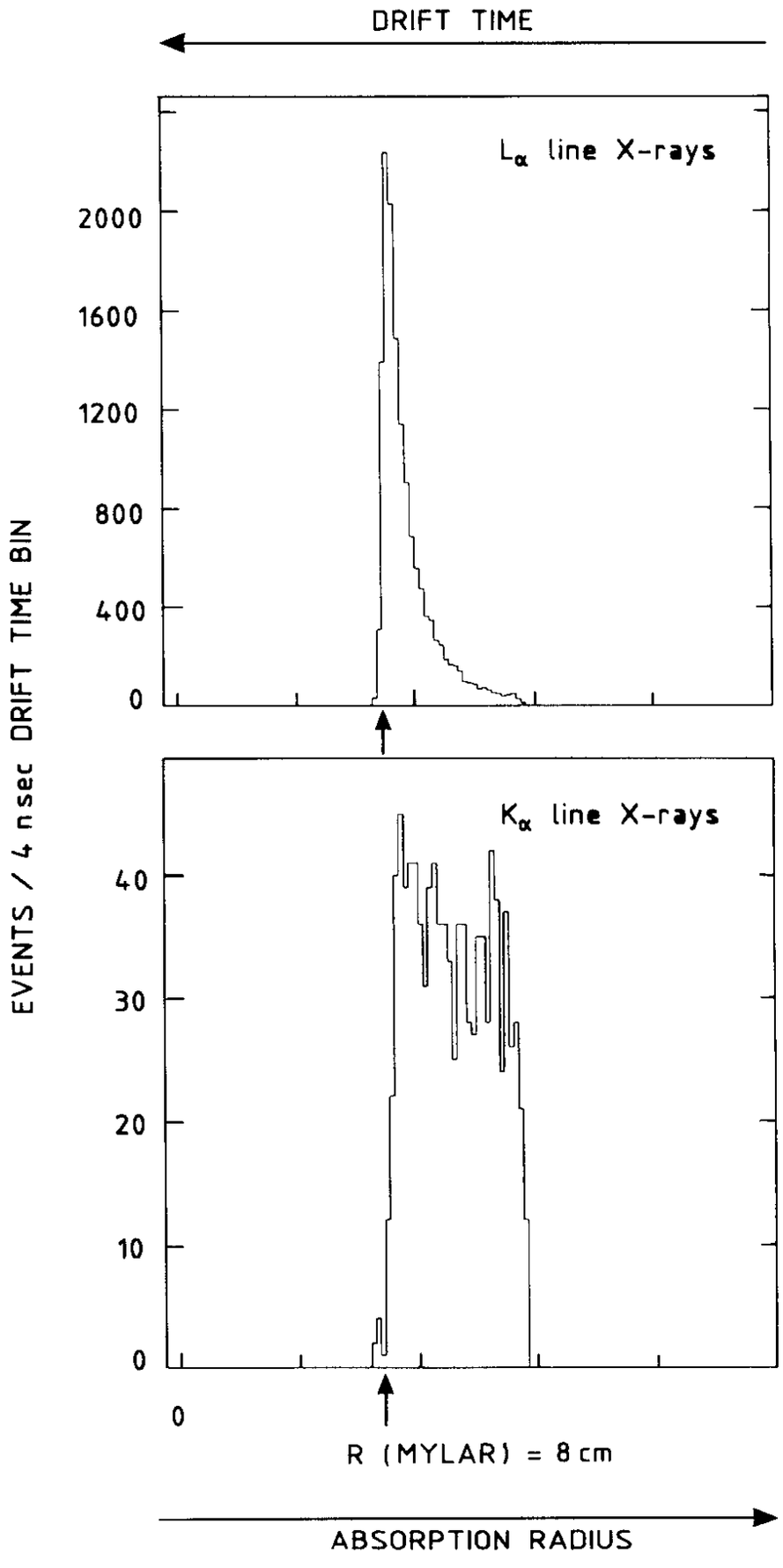
DRIFT TIME
L_α line X-rays
2000
1600
1200
800
400
0
K_α line X-rays
40
30
20
10
0
0
EVENTS / 4 n sec DRIFT TIME BIN
R (MYLAR) = 8 cm
ABSORPTION RADIUS

Fig. 6

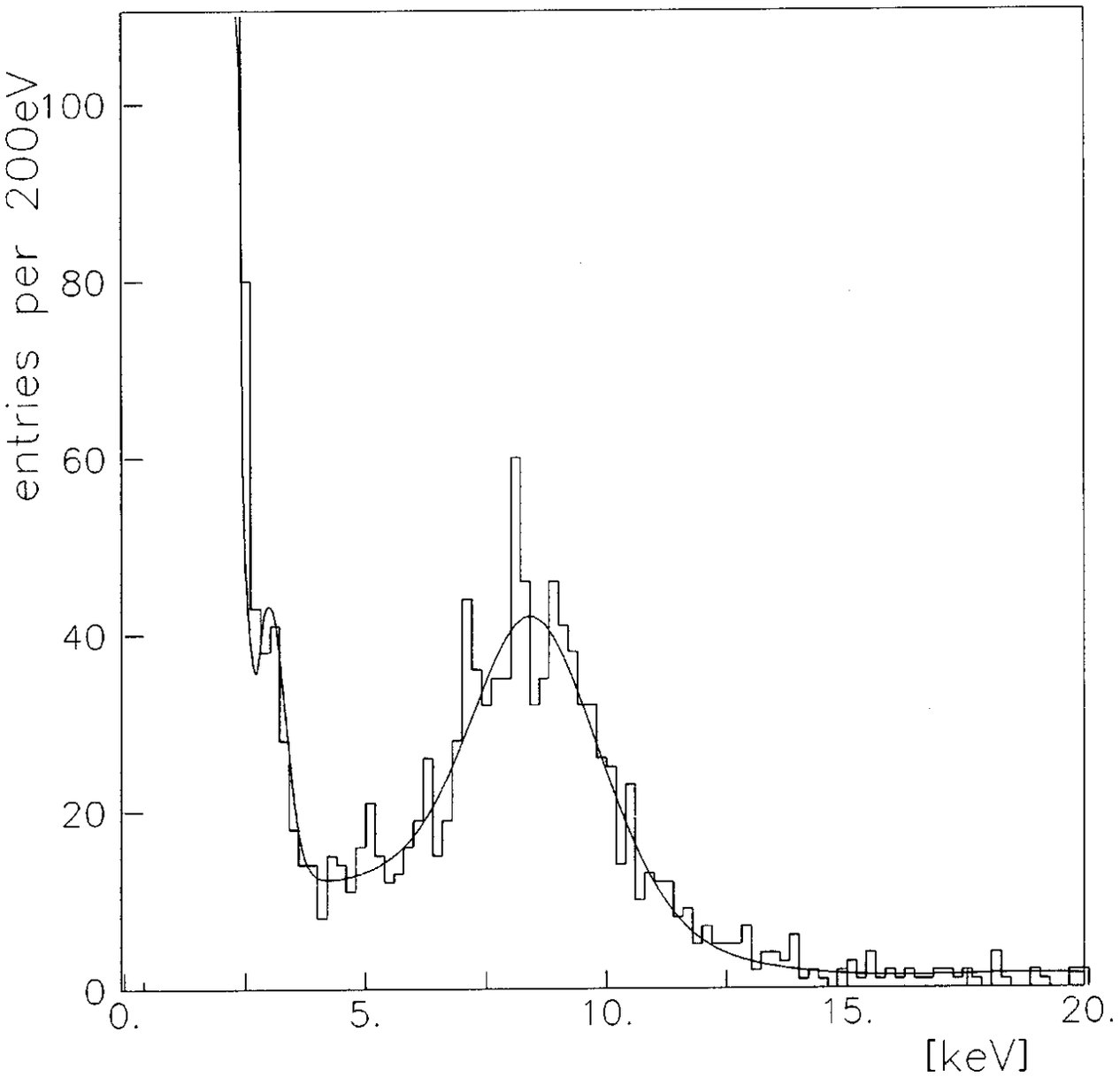

Fig. 7